

Article

Integrated Porosity Classification and Quantification Scheme for Enhanced Carbonate Reservoir Quality: Implications from the Miocene Malaysian Carbonates

Hammad Tariq Janjuhah ^{1,2,*} , George Kontakiotis ³ , Abdul Wahid ⁴ , Dost Muhammad Khan ⁴ ,
Stergios D. Zarkogiannis ⁵  and Assimina Antonarakou ³ 

¹ Department of Geology, Shaheed Benazir Bhutto University, Sheringal 18050, KPK, Pakistan

² Centre for Seismic Imaging, Department of Geosciences, University Technology PETRONAS, Sri Iskandar 32610, Malaysia

³ Department of Historical Geology-Paleontology, Faculty of Geology and Geoenvironment, School of Earth Sciences, National and Kapodistrian University of Athens, Panepistimiopolis, Zografou, 15784 Athens, Greece; gkontak@geol.uoa.gr (G.K.); aantonar@geol.uoa.gr (A.A.)

⁴ Department of Statistics, Abdul Wali Khan University Mardan, Mardan 23200, KPK, Pakistan; ab.wahid1996@gmail.com (A.W.); dostmuhammad@awku.edu.pk (D.M.K.)

⁵ Department of Earth Sciences, University of Oxford, Oxford OX1 3AN, UK; stergios.zarkogiannis@earth.ox.ac.uk

* Correspondence: hammad@sbbu.edu.pk or hammadtariq013@gmail.com



Citation: Janjuhah, H.T.; Kontakiotis, G.; Wahid, A.; Khan, D.M.; Zarkogiannis, S.D.; Antonarakou, A. Integrated Porosity Classification and Quantification Scheme for Enhanced Carbonate Reservoir Quality: Implications from the Miocene Malaysian Carbonates. *J. Mar. Sci. Eng.* **2021**, *9*, 1410. <https://doi.org/10.3390/jmse9121410>

Academic Editor: Markes E. Johnson

Received: 19 November 2021

Accepted: 7 December 2021

Published: 10 December 2021

Publisher's Note: MDPI stays neutral with regard to jurisdictional claims in published maps and institutional affiliations.



Copyright: © 2021 by the authors. Licensee MDPI, Basel, Switzerland. This article is an open access article distributed under the terms and conditions of the Creative Commons Attribution (CC BY) license (<https://creativecommons.org/licenses/by/4.0/>).

Abstract: The pore system in carbonates is complicated because of the associated biological and chemical activity. Secondary porosity, on the other hand, is the result of chemical reactions that occur during diagenetic processes. A thorough understanding of the carbonate pore system is essential to hydrocarbon prospecting. Porosity classification schemes are currently limited to accurately forecast the petrophysical parameters of different reservoirs with various origins and depositional environments. Although rock classification offers a way to describe lithofacies, it has no impact on the application of the poro-perm correlation. An outstanding example of pore complexity (both in terms of type and origin) may be found in the Central Luconia carbonate system (Malaysia), which has been altered by diagenetic processes. Using transmitted light microscopy, 32 high-resolution pictures were collected of each thin segment for quantitative examination. An FESEM picture and a petrographic study of thin sections were used to quantify the grains, matrix, cement, and macroporosity (pore types). Microporosity was determined by subtracting macroporosity from total porosity using a point-counting technique. Moldic porosity (macroporosity) was shown to be the predominant type of porosity in thin sections, whereas microporosity seems to account for 40 to 50% of the overall porosity. Carbonates from the Miocene have been shown to possess a substantial quantity of microporosity, making hydrocarbon estimate and production much more difficult. It might lead to a higher level of uncertainty in the estimation of hydrocarbon reserves if ignored. Existing porosity classifications cannot be used to better understand the poro-perm correlation because of the wide range of geological characteristics. However, by considering pore types and pore structures, which may be separated into macro- and microporosity, the classification can be enhanced. Microporosity identification and classification investigations have become a key problem in limestone reservoirs across the globe.

Keywords: carbonate reservoirs; porosity classifications; micro-macro-porosity; petrophysical properties; diagenetic processes; petroleum potential; grain sorting; sedimentary facies analysis; stratigraphic correlations; depositional environment

1. Introduction

Carbonate rocks account for 60% of the world's oil and gas reserves [1]. Most global oil reserves are in carbonate reservoirs [2–4]. These vast carbonate reserves are found in the Middle East, Libya, Russia, and Kazakhstan. Carbonate reservoirs are found in

large conventional oil fields such as Saudi Arabia's Ghawar [5]. Despite their reputation, carbonate reservoirs are no more difficult to predict, interpret, or define than siliciclastic reservoirs [6,7]. The diverse nature of carbonate reservoirs complicates their growth, making it difficult to determine their quality, particularly at inter-well scales [8]. It is more difficult to overcome poor recovery factors. When depositional geometry and diagenesis co-exist, very heterogeneous reservoirs are formed [9–11]. Carbonate succession stratigraphy, diagenesis, geochemical characteristics, and rock fabric variations influence development costs and ultimate recovery. Despite recent advances in stratigraphic and pore-scale carbonate reservoir characterization [12], numerous challenges remain in understanding and managing the uncertainties caused by heterogeneity. The use of modern petrophysics and computer modeling techniques simplifies solution development. Carbonate composition, diagenesis, microporosity prediction, microporosity effect on petrophysical properties, and depositional origins are yet unknown [13,14]. As a result, detecting carbonates is difficult since their characteristics vary within a reservoir.

These reservoirs, which have a permeability that is 1000 times greater than the surrounding rock matrix, might have a substantial impact on oil, gas, and water production [15,16]. To properly characterize carbonate deposits, quantitative physical parameters such as porosity and permeability must be considered. Because of their extreme variability, carbonate rocks are extremely difficult to identify, as shown by attempts to quantify petrophysical properties on different scales [17–19]. As a result of the enormous diversity of pore types, pore shape, and interconnectivity present in carbonates, little is known about their petrophysical properties. When working with carbonate reservoirs, poor relationships between porosity and other physical parameters such as permeability and sonic velocity are common [10].

The Central Luconia, offshore Sarawak, Malaysia research was used as a case study to address the limitations of several classifications. Malaysia's central Luconia carbonate reserves have great hydrocarbon potential. [20,21]. These carbonates contain 65 trillion cubic feet of gas and a modest oil deposit, making them commercially important [17]. Because it is a significant hydrocarbon province, the province of Luconia offshore Sarawak is a critical geological unit for understanding Malaysia's distribution of hydrocarbon resources. According to Janjuhah, Alansari, Ghosh and Bashir [21] commercial levels of an unrelated gas have been discovered in 56 carbonate platforms. These reservoirs are often associated with grain-rich facies types.

The main objectives of this research are to develop a qualitative understanding of carbonates, to highlight the challenges of current porosity classifications used in industry to identify carbonate reservoir properties, and to further emphasize the importance of categorizing the porosity classification, using a Miocene carbonate reservoir rock as an example.

2. Limitations of Existing Porosity Classifications and their Texture

Folk [22] was the first to attempt to analyze the differences in limestone texture and propose a classification scheme. Folk [22] divided limestone into three types (allochems, microcrystalline ooze, and sparry calcite cement) (Figure 1), as well as eight textural types (Figure 2). Furthermore, Folk [22] coined the concept "allochem," which refers to chemical precipitation. In geology, the allochems' synonyms, "common chemical precipitation," do not have the same meaning as in pure chemistry. Rock complexes with a higher degree of order, which have been subjected to significant movement, may be found in geology. Based on their importance in carbonate rock, Folk divided allochems into four classes (intraclasts, oolites, fossils, and pellets). The allochems that make up the majority of limestone are reflected in the rock structure and non-skeletal grains. A clay-sized matrix is represented by the microcrystalline ooze. The sparry calcite cement, on the other hand, fills the pore spaces and leaves empty pores after the microcrystalline ooze has been washed away. Microcrystalline ooze and sparry calcite cement are fundamental features of rocks, Folk claims, based on their proportions.

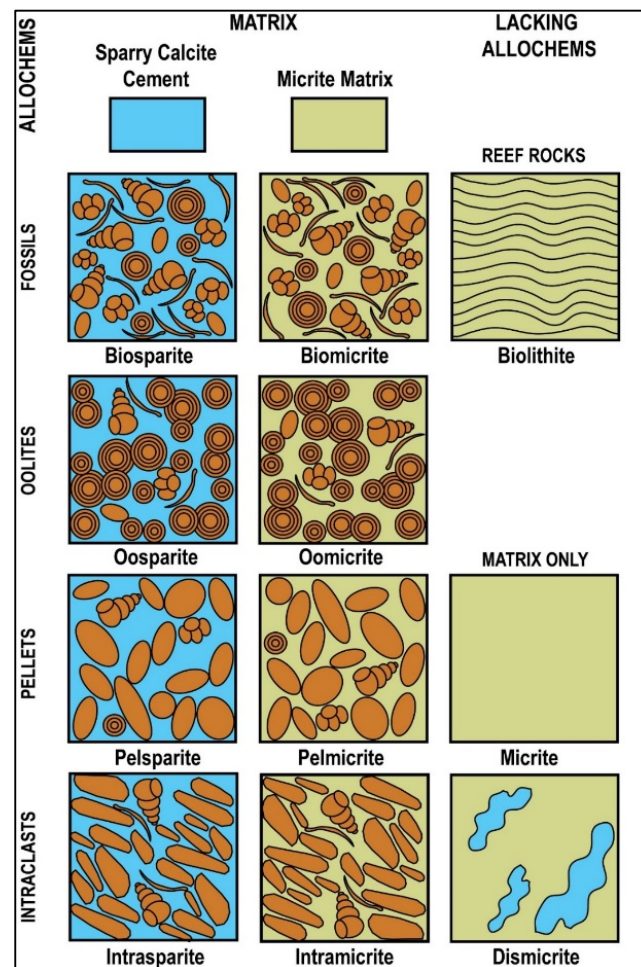


Figure 1. Representing the Folk classification of limestone, based on alluvial micrite matrix and sparry calcite cement.


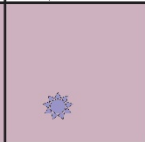
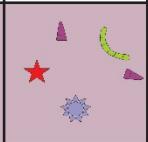
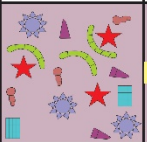
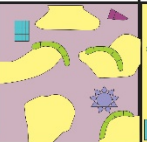
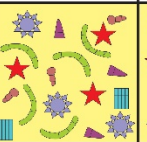
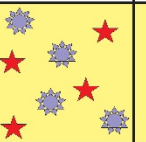
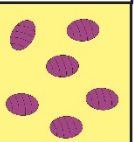
>2/3 Micrite Matrix					Subequal Micrite/ Spar	>2/3 Spar Cement		
% Allochems	<1%	1-10%	10-50%	>50%		Poor Sorting	Good Sorting	Rounded & Abraded
<div>←———— Low Energy, Quiet Water Settings High Energy Waves and Currents ———→</div> <div>←———— Matrix-Supported Allochems Grain-Supported Allochems ———→</div>								
Rock Name	Micrite	Fossiliferous Biomicrite	Sparse Biomicrite	Packed Biomicrite	Poorly Washed Biomicrite	Unsorted Biosparite	Sorted Biosparite	Rounded Biosparite
								
Terrigenous Classification Analogues	Claystone		Sandy Claystone	Clayey or Immature Sandstone		Sub-mature Sandstone	Mature Sand	Supermature Sand

Figure 2. Folk classification of limestones based on textural parameters and implied depositional conditions.

Folk [22] also indicated that the textural structure of limestone had matured (Figure 2). Based on the ratio of grain- and mud-supported grains, this textural maturity is classified into eight groups. He employed a descriptive textural maturity classification, however, he left out certain genetic implications and repercussions. A thin section investigation is most suited to Folk [22] classification. Folk [22] suggested that micritic formation could be an exception to the norm. Lime mud may develop in a high-energy zone, if not eliminated by algae and waves. Sparite can only grow in a protected environment, such as a lagoon full of accumulating fossils. As a result of their chemical interaction, lime mud was not formed by precipitation.

However, since it is a well-known carbonate, the Dunham [23] rock classification, which was modified by Embry and Klovan [24] to enhance carbonate reef textures, is frequently used in the petroleum sector (Figures 3 and 4). This approach works well in explaining rocks using a hand lens or binocular microscope. If the limestone grains are close together and there is no mud present in the sediment, the sediment is referred to as a grainstone. A packstone is a carbonate that is grain-supported and contains a small quantity of mud. The sediment is referred to as a wackestone if it is mud-supported yet contains more than 10% grains, while it is referred to as a mudstone if it contains less than 10% of grains. Folk [22] refers to carbonate mud-rich rocks as micrites, although Dunham [23] refers to them as mudstones or wackestone. “Grainstone” and “packstone” are terms used by both Folk [22] and Dunham [23] to describe rocks with a small matrix. Dunham’s [23] classification was expanded by Embry and Klovan [24], who included coarse-grained carbonates. A wackestone with grains of a size greater than 2 mm has been renamed as floatstone, while a coarse grainstone is referred to as rudstone in the relevant scheme. However, applying these methodologies to ancient limestones is difficult because of the limits placed on the ability to judge an organism’s function by diagenesis and sample size.

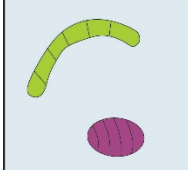
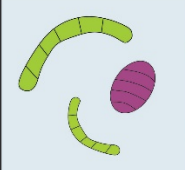
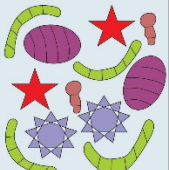
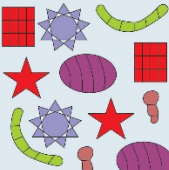
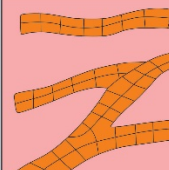
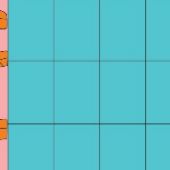
Original Components not Bounded Together During Deposition				Original Components Bound Together	Depositional Texture not Recognized
Contains Lime Mud		Grain-Supported	Lacks Mud and is Mud Supported		
Mud-Supported					
Less than 10% grains	More than 10% grains				
Mudstone	Wackestone	Packstone	Grainstone	Boundstone	Crystalline
					

Figure 3. Representing the Dunham classification of limestone based on depositional texture.

Allochems not Originally Bound During Deposition						Autochems Bound During Deposition				
Clasts >2 mm make up <10%						Clasts >2 mm make up >10%				
Contains lime mud (0.03 mm)			No Lime Mud			Matrix Supported	Supported by Clasts >2	Organisms Acts as Baffles that Trap sediment	Organisms that Enerust an Bind e.g., Algal Mats, Calcareous Algae, Bryozoans	Organisms that Build Rigid Structures e.g., Corals, Stromatoporoids, Poroids, Oyster Buildups
Mud Supported Frameworks		Clast Supported Frameworks								
<10% grains <2 mm	>10% grains									
Components of Dunham's Classification						Floatstone	Rudstone	Bafflestone	Bindstone	Framestone

Figure 4. Representing the extended classification of limestone based on depositional texture.

Porosity Classifications

Carbonate rock has a broad range of pore sizes, and the network of connections within the rock is often complicated. There is usually a lack of correlation between porosity and other physical parameters such as permeability and velocity. Understanding how carbonate reservoirs form porosity is critical [25–28]. The structure of the pores has a significant influence on permeability and elastic properties [10,29,30]. Various rocks with the same porosity but varying permeability and acoustic velocity may be encountered [31]. The pore structure of carbonate rocks has been shown to affect the petrophysical properties in many studies [32–39]. Most studies support a dual-porosity model, since geologists and petrophysicists are unable to agree on how to define pore types. [31,40–44].

Archie [45] was the first to investigate the link between rock fabric and petrophysical parameters, highlighting the relevance of pore structure in defining pore types. Table 1 shows the matrix texture and pore type visibility used in the Archie [45] classification (Table 2).

Choquette and Pray [26] developed a descriptive classification scheme for carbonate pore types that is widely accepted and used in both the commercial and academic sectors. The majority of the system's genetic classification is made up of primary and secondary pore systems (Figure 5; Table 3). Intergranular pore spaces, which are frequent in terrigenous sand, are the major source of porosity [26,46]. Only one aspect of the carbonate pore system is shared with terrigenous sand. Primary pores occur within the skeletal chambers, and are well-protected by enormous skeletal framework textures, due to the diversity of carbonate grains and sediment texture. The preservation of primary pore systems depends on a variety of factors when a sediment is turned into limestone [26]. The majority of pores in carbonate rocks, on the other hand, are secondary pore systems in nature [26,47,48].

When carbonate sediment is deposited, it creates primary porosity [26,49]. In 1970, researchers Choquette and Pray [26] coined a term to characterize porosity's origins; its size, shape, and abundance. Cementation and dissolution are two ways of tracing the genesis. Carbonate sands and gravels lose their porosity due to the precipitation of cement and compaction [26,46,50,51]. Secondary porosity develops after the sediment has been deposited [26,28,49]. In this stage of diageneses, a variety of chemical and mechanical activities take place, including the conversion of carbonate sediment to limestone or the

modification of limestone pores [26,28,52,53]. In addition to the fabric-selective secondary pores, there are also non-fabric-selective secondary pores [26].

Secondary pores that are fabric-selective are linked to the sediment or rock's initial textural components [26]. Moldic porosity is a prevalent form of pores in a fabric-selective dissolution [54]. Due to the dissolution of skeletal or nonskeletal grains, the grain mould changes into pores, resulting in this structure [26,28,46,49]. It is also typical to find inter-crystalline porosity between crystals that have developed in situ by recrystallizing or, more often, through dolomitization. Limestone's non-fabric secondary pores are unconnected to the limestone's textural components [26,28,49]. These pore systems crosscut the limestone's texture, such as fractures, vugs, and so on.

Table 1. Micrite texture Archie classification of carbonate rock.

Matrix Texture	Hand Sample Appearance	Microscopic Appearance
Type-I Compact Crystalline	Edges and surfaces that are both sharp and smooth.	The splitting of clusters of crystals in thin flanks produces “feather edges” in a matrix made up of crystals weakly interacting but with no obvious pore spaces between them.
Type-II Chalky	The small crystals are less closely interlocked and hence reflect light in diverse directions, or, because the material is composed of very fine granules, a dull, chalky, crystalline appearance is missing.	Less interlocking crystals interlock at various angles. This may cause a chalky texture, although others may become crystalline.
Type-III Granular	Sugary appearance (Sucrose). Very fine: 0.05 mm, Fine: 0.1 mm, Medium: 0.2 mm, Coarse: 0.4 mm.	Crystals interlocking at varying angles, allowing for significant porosity between crystals. This includes oolitic textures.

Table 2. Visible pore size classification of carbonate rock.

Class	Description
Class A	Pores smaller than 0.01 mm in diameter, not visible with a 10× resolution microscope.
Class B	Greater than or equal to 0.01 mm of visible porosity
Class C	More than 0.1 mm of visible porosity, however, the mess is less than the size of the cuttings
Class D	Secondary crystal development on the cutting surfaces, or “weathered-appearing” faces displaying signs of fracture or solution channels, is an indication of visible porosity.

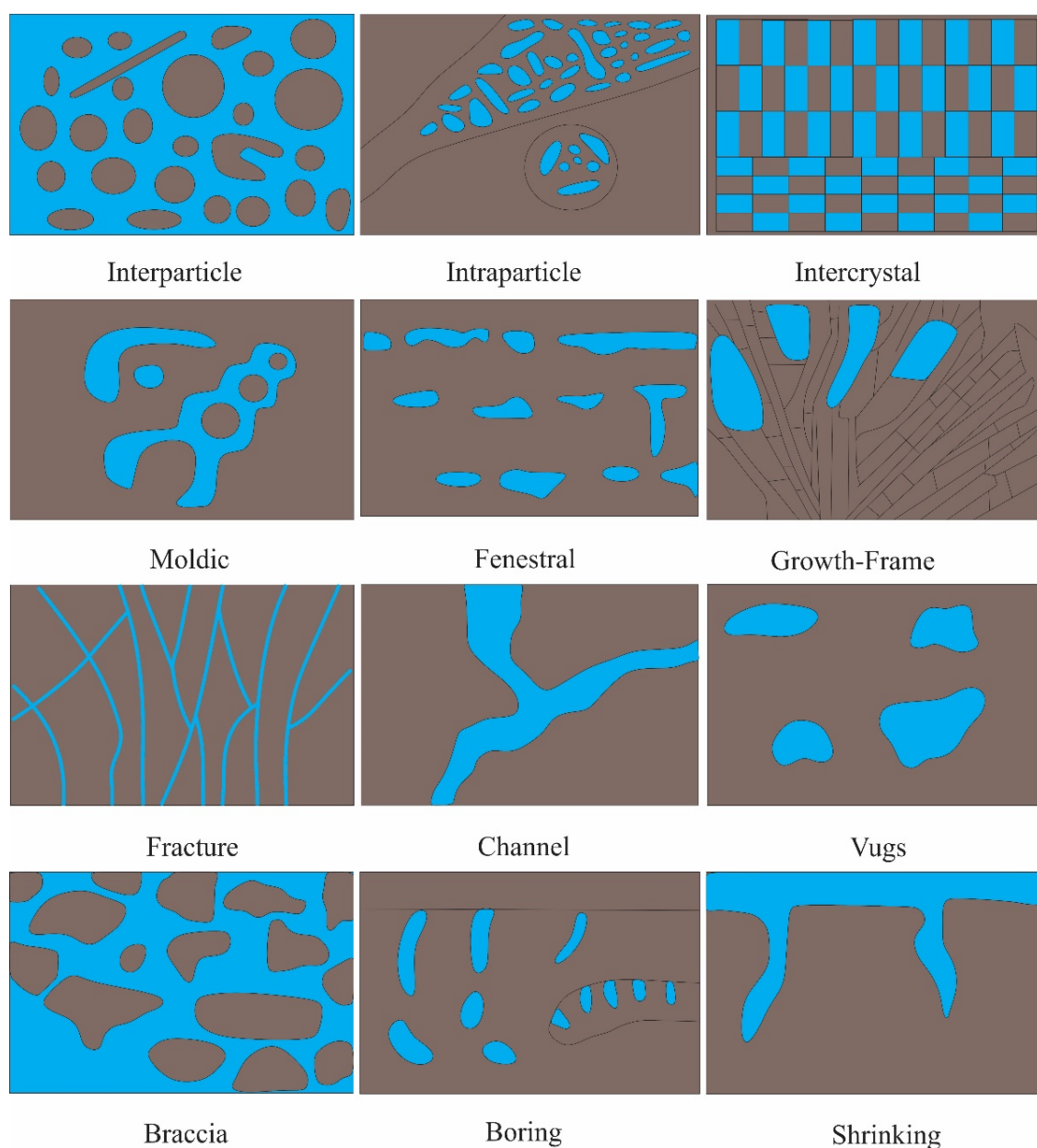


Figure 5. Choquette and Pray classification of limestone porosity.

The Lucia [38,55], classification uses both the Dunham [23] texture classification and the Choquette and Pray [26] classification to address the fundamental geological factors that reduce the uncertainty of petrophysical parameters of carbonate geological models. Lucia [38]’s classification is primarily composed of interparticle pores and vuggy pores. When applied to a geological model, the Archie [45] classification is still useful in determining petrophysical properties, but it does not provide comprehensive information regarding deposition and diagenetic processes. Dunham [23] and Choquette and Pray [26] classifications are also used often, according to Lucia [38]. Nonetheless, neither can be easily linked to quantitative reservoir properties that indicate the wellbore’s local environment.

In an effort to close the gap, Lucia [38] presents a method for obtaining the basic mappable geological properties that allow for the petrophysical quantification of geological reservoir models. The Lucia [38] classification, controls permeability and saturation. Texture [23], grain size, pore type, and distribution are all factors that influence rock fabric. Grain-dominated, muddy grain-dominated, and mud-dominated are the three elements

that make up the texture (Figure 6). The only two pore-size classes in the simplified Lucia [38] classification are intraparticle separated vugs and touching vugs.

Table 3. Description of porosity classification of limestone.

Interparticle	Between the grains, there is a space. The permeability and recovery of sand are generally excellent. Porosity and permeability are reduced due to the use of interparticle cement.
Intraparticle	Within particles, there is an area known as a pore space. The pore size and permeability of a fossil chamber, such as a foram's chamber, or a coral microstructure, determines its porosity and permeability. Water or oil in smaller pore networks may be irreducible.
Intercrystalline	Between the crystals of recrystallized limestone, there is porosity. The most prevalent kind of porosity in dolomites, which are often very porous and permeable reservoirs. If present in chalk mudstone, porosity may be significant due to the presence of a large amount of irreducible water, whereas permeability will be low until fractured.
Moldic	Porosity occurs when skeletal and non-skeletal grains leach. Effective porosity and permeability are determined by the texture, the degree to which grains leach, and the quantity of interparticle cement. Generally inefficient porosity and poor permeability when just isolated pore types are present, but great when inter-crystal or interparticle pore types are present.
Fracture	Porosity formed by the brittle deformation of rock. Porosity is usually low, but permeability will be higher.
Vugs	Porosity formed by an enlargement of fabric-selective pore such as moldic and intraskeletal pores.
Channel	Porosity formed by enlarged dissolution of early formed pore system.





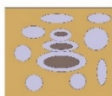
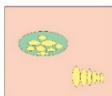


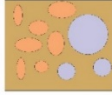



Vuggy Pore Space								
Separate-Vugs Pores (Vug-to-matrix-to-vug connection)				Touching-Vug Pores (Vug to vug connection)				
Percent Separate Vug Porosity	Mud-Dominate Fabric		Grain and Mud-Dominate Fabric					
	Example Types		Example Types					
	Moldic pores		Moldic pores		Cavernous		Fractures	
	Intrafossil pores		Intrafossil pores		Braccia		Solution-enlarged fractures	
	intragrain micropores		intragrain micropores		Fenestral		Microfractures connect moldic pores	

Figure 6. Geological and petrophysical classification of vuggy pore spaces based on vugs interconnection, after Lucia [38].

Lønøy [42] proposed a new classification of pores based on the nomenclature of Lucia [38] and Choquette and Pray [26] descriptive. There were 20 distinct types of pores for Lønøy [42]. It is feasible to attain good access to sedimentological and diagenetic properties of a sample using the Lønøy [42] classification. Unlike Lucia [38], Lønøy [42] emphasized that pore size, not grain size, is used to classify his samples. The Lønøy [42] classification is useful for working with a small data set, but it is not ideal for a huge dataset. To differentiate between macro and micropores, microporosity was previously included in

the classification. Microporosity is present in several carbonate deposits across the world. Cantrell and Hagerty [41] and Janjuhah, Alansari and Vintaned [10] conducted extensive research on Middle East carbonates. With regard to microporosity definition, academics have differing viewpoints. Geologists, petrophysicists, and geophysicists have all reported microporosity in the literature. In this study, micropores were defined as pores with a diameter of less than 10 µm [31,56–59]. The addition of micropores to a reservoir has no effect on fluid migration and increases the risk of underestimating the reservoir's quality.

3. Application of Macro-Micro Classification from Miocene Carbonates

Material and Methods

Central Luconia's carbonate rocks from Cycle V are the focus of this research. To explain the core analysis, data was manually plotted onto a 1:40 scale core description sheet. This section focused on describing a variety of sedimentological properties, such as depositional textures, the nature of skeletal and non-skeletal grains, lithology, and diagenetic features such as leaching, stylolites, and visible porosity (Table 4). By examining the core, several lithofacies were identified.

Table 4. Flow of core description for this study.

Core Description Sheet	Grain Size	Lithology	Depositional Texture	Leaching	Stylolite Frequency	Visual Porosity Distribution
Resources	Wentworth [60]	HCL, Grain Density	Dunham [23] (Figure 4)	Visual Observation	Park, 1968	Visual Observation

The porosity, permeability, and grain density of the core were measured using 142 core plugs. Under transmitted light, 53 thin thin-sections were prepared and examined subjectively and statistically from these core plugs, and 700 counts per sample employed a point-counting technique (J. Microvision) to analyze thin sections' grains, matrix, cement, and visible porosity. Weger, Eberli, Baechle, Massaferrero and Sun [35] developed the Digital Image Analysis (DIA) technique, which assesses microporosity, using four photographs to represent the whole thin section (Figure 7). However, due to the poor quality of the photographs, there is a significant amount of uncertainty. Each thin section in the present research is covered by 32 high-resolution petrographic images, which are combined into a photo panel in order to estimate the level of macroporosity, reducing the uncertainty associated with pore geometry variation (Figure 7). This means that any zone that falls below the threshold value will be colored red, indicating a zone with a high number of micropores. The entire red region is made up of very microporous sections, signifying the ideal areas. Macroporosity characterized pores with a diameter of greater than 10 µm. Total porosity was determined by injecting helium at 1800 to 2000 psi pressure into the sample using Vinci Technologies' poro-perm apparatus. Thin sections were utilized to quantify macroporosity, which was then deducted from the total porosity calculated from the core plug.

$$\text{Microporosity} = \text{Total porosity (central plug)} - \text{Macroporosity (thin section)}$$

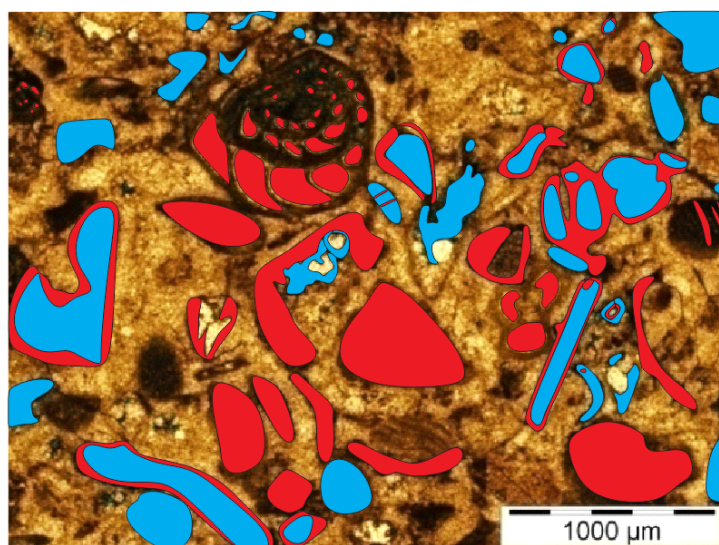


Figure 7. False color DIA image of mouldic, vuggy and intraparticle porosity developed in foraminifera and different bioclasts in Well A. Total porosity is 19%, the blue color represents macropores which are 8.5%, whereas red color represents microporosity which is 10.5%.

The well-observed pore types were found to be isolated in nature. Central Luconia carbonates were highly leached, causing partial or total disintegration of the basic rock structure and the formation of an expanded isolated molded porosity.

4. Results and Discussion

4.1. Facies Analysis

To describe the lithofacies, the standard terminology was used as provided by Janjuhah et al. [61]. They identified eight different lithofacies for Central Luconia carbonates, based on depositional texture and wireline-log response (Table 5) as follows: Coated Grain Packstone (F-1), Massive Coral Lime Grainstone (F-2), Oncolite Lime Grain-dominated Packstone (F-3), Skeletal Lime/dolo Packstone (F-4), Coral (p) Lime Mud dominated Packstone (F-5), Coral (B) Lime dominated Pack-Grainstone (F-6), Cross-Bedded Skeletal Lime Packstone (F-7) and Bioturbated Carbonate Mudstone (Chalk F-8). This work uses the facies system devised by Janjuhah, Salim, Mohammad, Ali, Ghosh, Hassan and Hakif [17].

According to facies scheme of Janjuhah, Alansari and Santha [9] and Janjuhah, Salim and Ghosh [61], five facies were identified in the studied well namely: Coated Grain Packstone (F-1), Massive Coral Lime Grainstone (F-2), Oncolite Lime Grain Dominated Packstone (F-3), Skeletal Lime Packstone (F-4) and Platy Coral Lime Mud Dominated Packstone (F-5) (Figure 8; Table 5).

Table 5. Lithofacies for Central Luconia carbonates based on depositional texture and wireline-log response (adopted from Janjuhah et al. [9]).


Lithofacies		Description
FA-1 Coated Grain Packstone		Texture: packstone (floatstone) Mineralogy: limestone Components: algae >50%, oncolite algae <40%, corals <30%, separate vugs, skeletal debris (angular—subangular), forams, echinoderms, gastropods, leaching Grain size/sorting: fine-medium gravel/moderately—poor

Table 5. Cont.

Lithofacies		Description
<p>FA-2 Coral (m) Lime Pack-Grainstone</p>		<p>Texture: packstone–grainstone (rudstone) Mineralogy: limestone Components: corals (m) >50% (up to 8 cm in diameter), platy coral up to 20%, branching corals (15%), solitary coral <5%, algae, disconnected vugs, oncolite algae, skeletal grains (angular-subangular), gastropods, bivalves, echinoid spines Grain size/sorting: very coarse-granule/moderately poor</p>
<p>FA-3 Oncolite Lime Grain-dominated Packstone</p>		<p>Texture: packstone (rudstone) Mineralogy: limestone Components: oncolite algae >70% (diameter 2 to 6 cm), stylolite, corals >30%, separate vugs, algae, gastropods, bivalves, echinoid spines, skeletal grains (angular-subangular), leaching Grain size/sorting: medium-gravel/moderately poor</p>
<p>FA-4 Skeletal Lime/dolo Packstone</p>		<p>Texture: packstone (floatstone-rudstone) Mineralogy: limestone—dolomitic limestone Components: skeletal debris >60% (angular-subangular), bivalves, isolated gastropods, corals (m) <20%, Coral (p) <15%, leaching Grain size/sorting: fine-coarse grain/moderately well sorted</p>
<p>FA-5 Coral (p) Lime Mud dominated Packstone</p>		<p>Texture: packstone (floatstone) Mineralogy: limestone Components: rich platy corals >70%, solitary coral up to 15%, algae, small fractures, disconnected small vugs, skeletal debris (angular-subangular), gastropod, forams, echinoid spines Grain size/sorting: fine-coarse/poor</p>
<p>FA-6 Coral (B) Lime dominated Pack-Grainstone</p>		<p>Texture: packstone-grainstone (floatstone) Mineralogy: limestone-dolomitic limestone Components: branching coral 50%, 20% red algae, 15% forams, 5% massive coral, 5% bivalve, 5% other skeletal debris (angular-subangular) Grain size/sorting: very coarse-granule/poor</p>
<p>FA-7 Cross Bedded Skeletal Lime Packstone</p>		<p>Texture: packstone (floatstone) Mineralogy: dolomitic limestone to limestone Structures: graded bedding Components: forams 65%, red algae 10%, coral fragments 10%, bivalve 5%, echinoderms 5%, other skeletal debris 5% Grain size/sorting: very coarse-pebble/poorly or moderately sorted</p>

Table 5. Cont.

Lithofacies	Description
<p>FA-8</p> <p>Bioturbated</p> <p>Carbonate Mud stone (Chalk)</p>	<p>Texture: wackstone—packstone</p> <p>Mineralogy: dolomitic limestone</p> <p>Structures: bioturbation</p> <p>Components: burrowing & bioturbation 60%, forams 10%, coral debris 10%, red algae 5%</p> <p>Grain size/sorting: very fine-coarse/moderately well sorted</p>

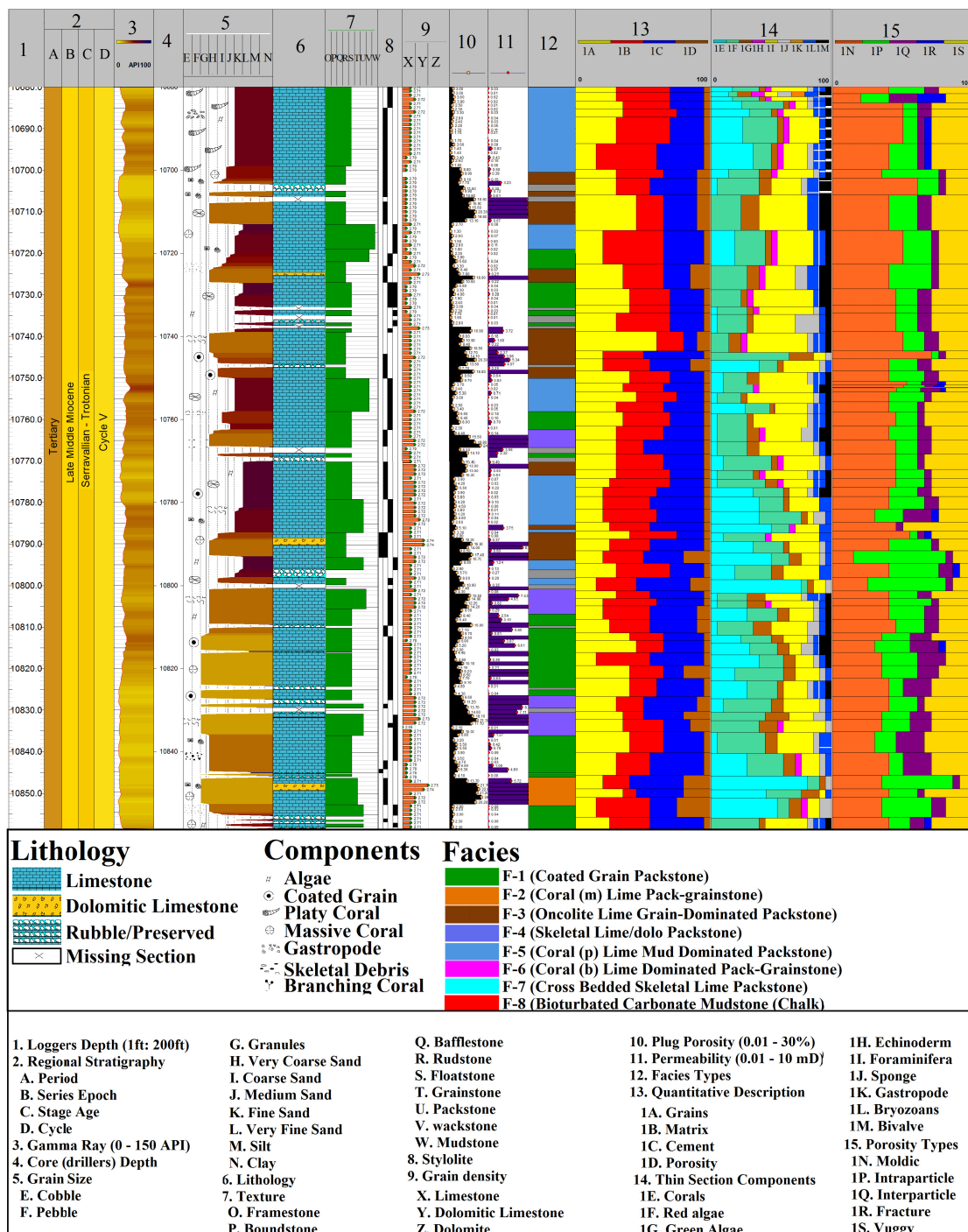


Figure 8. Sedimentological log is showing the qualitative and quantitative description of Well A in Central Luconia, offshore Sarawak, Malaysia.

4.2. Pore Types

The pore system in Central Luconia is dominated by isolated vugs [38,62]. The main rock fabric is thought to have been leached by skeleton allochems, resulting in partial or full dissolution. Carbonate mineralogies such as aragonite and high-magnesium calcite (corals and green algae, some echinoderms, bivalve, and sponges) were very unstable and dissolved quickly after burial, resulting in the selective breakdown of these organisms' skeletons [63]. Moldic pores were predominant in the thin section, according to first impressions (Figures 8 and 9). The porosity of mould was increased; however, it was not well-connected (Figure 9). Various pores can be observed, including moldic, intraparticle, interparticle, fractured, and vuggy porosity, according to the Choquette and Pray [26] classification (Figure 9). The observable pores are almost all secondary in origin.

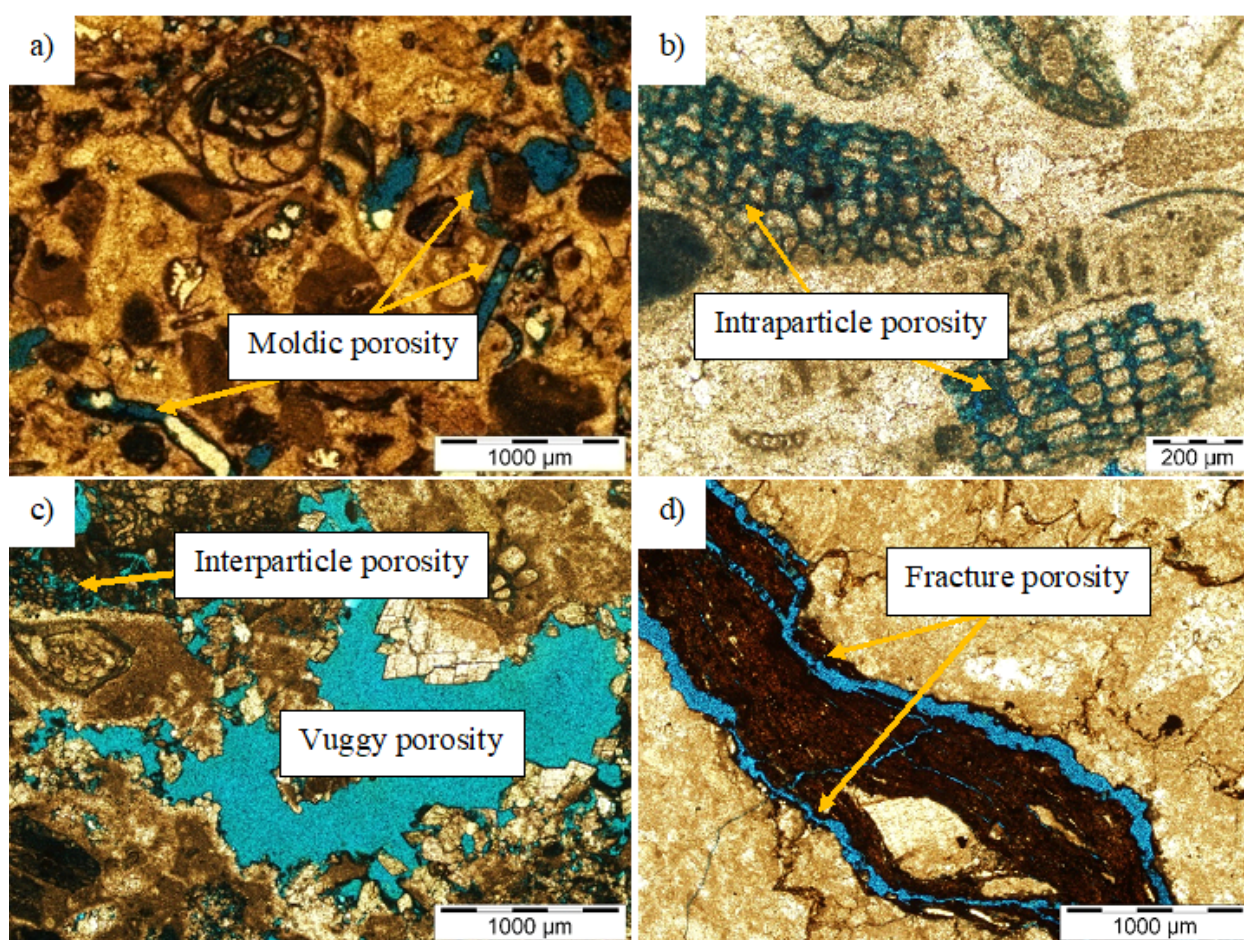


Figure 9. Photograph representing the different types of porosity (a) Intraparticle and mouldic porosity, (b) Fracture porosity, (c) Vuggy porosity and (d) Interparticle porosity and partial filling of dolomite, dolomite cement filling pore spaces and the rate of dolomitization increases with the time in Central Luconia, offshore Sarawak, Malaysia.

Facies 4 (F-4) dominates the five facies, accounting for 45% of the cored intervals, followed by 25% for Facies 1 (F-1), 15% for Facies 5, 10% for Facies 3, and 5% for Facies 2. (Figure 8). The thin sections are dominated by grain, which occupies 35% of the total area, followed by 30% matrix, 30% cement, and 5% porosity, as can be seen in Figure 8. Eight major grains are observed in Well A Central Luconia, offshore Sarawak, Malaysia (Figure 9). Coral, sponges, echinoderms, bivalve and bryozoans, and foraminifera make up most of the grains (Figure 8). Figure 3 shows that mouldic porosity is the most common, accounting for 50% of the total interval, followed by vuggy porosity (20%), intraparticle porosity (15%), interparticle porosity (10%), and fracture porosity (5%), respectively (Figure 8).

4.3. Quantification of Macro-Microporosity

To determine the presence of microporosity, the macroporosity of carbonate rocks was measured. When the diameter of moldic, intraparticle, interparticle, and vuggy pores exceeds 10 μm , they are identified as having macroporosity. The abundance of macroporosity was determined using two methods. Point counting and a digital image analysis with a threshold setting were used to collect data on macroporosity. DIA was utilized to produce a false-color image, based on the photomicrograph of each thin section to examine macroporosity distribution (Figure 7). The porosity of core plug measurements varies between 3% and 25% (Figure 8). The total porosity of a core-plug sample was subtracted from the macroporosity observed in the thin section analysis to calculate the microporosity values (point counting and DIA). In Central Luconia, most of the microporosity is located in limestone, and these pores are found between the cement of calcite microcrystals. Understanding the distribution and measurement of microporosity is critical when dealing with carbonates. Porosity in the core plug does not adequately account for fluid flow because the pore bodies have different pore throats. These pore throats have a detrimental influence on fluid flow [31,35,64,65]. According to this research, carbonate reservoir models overestimate matrix porosity, which has a major impact on reservoir evaluation. Moldic and vuggy porosity are frequently used in carbonate reservoir models, but matrix porosity is underestimated, which has a substantial impact on reservoir assessment. Depending on their size, these pores are classified as macropores or micropores. We studied the occurrence and distribution of microporosity in Central Luconia, since pores are divided into macropores and micropores (Figure 7). Cantrell and Hagerty [41], Anselmetti et al. [66], Ruzyla and Jezek [67], Yanguas and Dravis [68] and Milliken and Curtis [69], all agree that the quantitative observation of pore types on blue-impregnated thin sections is an effective method for improving the ability to detect the microporosity zone.

Following Lambert, Durllet, Loreau and Marnier [2], Kaczmarek, Fullmer and Hasiuk [59], Lucia [62], Pittman [64], Arribas et al. [70], Cox et al. [71], Flugel [72], Kaldi [73], Volery et al. [74], Morad et al. [75] and our observations, carbonate allochems are found to be frequently less porous than carbonate matrix material. According to Cantrell and Hagerty [41], the quantity of mud in limestone impacts the degree of microporosity and overall porosity. As mud content increases, the proportion of microporosity increases, resulting in a reduction in overall porosity. We observed that microcrystals are more abundant in foraminifera, coral, red algae, and sponge grains than in echinoderms, bivalves, and bryozoan grains, in our thorough investigation (Figure 10). Carbonate allochems are found to be less permeable than carbonate matrix material in the initial observation. Microcrystal concentrations are greater in foraminifera and red algae (Figure 10). Lucia and Loucks [43] also explicitly noted that forams, coral, and red algae contain more microcrystalline than echinoderms and bivalves. Dissolution pits and micro-fractures can include micron and submicron-sized pores, although they are less common. Micro- and submicron-scale pores in microporous limestone contribute less to overall porosity than inter-crystalline pores found in matrix and carbonate allochem [41].

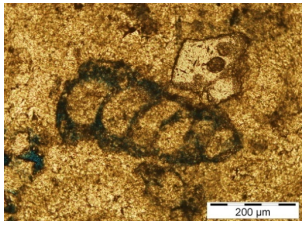
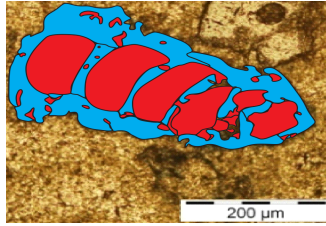
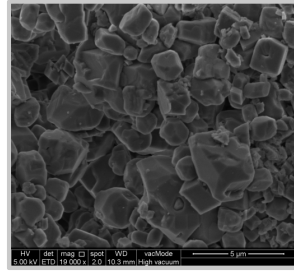
Components	Microporosity in Component	FESEM Image of Component
		
Foraminifera	Microporosity Percentage: 53%	

Figure 10. A systematic evaluation of microporosity in carbonate allochems (e.g., Foraminifera), Central Luconia, offshore, Sarawak, Malaysia.

4.4. Effect of Microporosity on Petrophysical Properties

Microporosity measurements show that the Miocene carbonates have an appropriate amount of microporosity, which may account for as much as 40–50% of the total porosity (Figure 11). Deposition and diagenesis are linked to the presence of this microporosity. Miocene carbonate build-ups in the studied Well-A underwent various episodes of diagenetic alterations, including micritization, cementation, compaction (physical and chemical), dissolution, and dolomitization, according to [9]. These diagenetic processes have specific alteration conditions that correspond to the changes that occur during the time. In their study, they claimed that micritization and calcite cementation impact reservoir quality and, in particular, carbonate rock permeability in the majority of cases. The higher the amount of microporosity, the more the area is micritized and cemented. Microporosity, on the other hand, reduces as dissolution increases [14,75]. Because transmitted light microscopy has a low resolution, this phenomenon was further confirmed using FESEM (Field Emission Scanning Electron Microscopy) images, which clearly revealed the micropores (Figure 12). In Well A, the degree of microporosity varies between 20 and 60%. The existence of macroporosity in different facies is related to the dominance of microporosity in Central Luconia, because each sample represents a distinct pore type, and these pore types are altered by various diagenetic processes.

The depositional texture is important in the development of microporosity. The microporosity of a rock sample is mostly controlled by the depositional textures as a whole. The proportion of microporous components increases as the depositional texture becomes muddier, increasing the abundance of microporosity in Central Luconia, offshore Sarawak, Malaysia. The floatstone and packstone depositional textures are dominated by grains with significant moldic porosity (large macropores), with small micropores present in the matrix (Figures 9–12). The positive contribution towards the quantification of microporosity is mostly limited to microporous grains, however, cement and matrix with micropores may also be present, but their contribution towards the quantification of microporosity generally are not considered in Central Luconia, as most of the core and thin sections revealed that the carbonate in Central Luconia is grain- rather than mud-dominated. The depositional texture of mudstone and wackestone is quite rare. The microporosity of these rocks (floatstone and packstone) is relatively high, ranging between 20 and 60% of total porosity (Figures 10–12). Macroporosity is less abundant in mud-dominated carbonate rocks because intraparticle and interparticle porosity is widespread and they are filled by the microporous matrix, resulting in reduced macroporosity but increased microporosity (Figures 11 and 12). The microporous matrix is abundant in mud-supported grains (Facies-1 and Facies-5) since macroporosity is often quite low. Microporous grains provide from 70 to 80% of the total porosity of these mud-supported grains (Facies-1, Facies-5). As

pore spaces are filled with microporous grains and the microporous matrix, the percent of microporosity rises in total porosity.

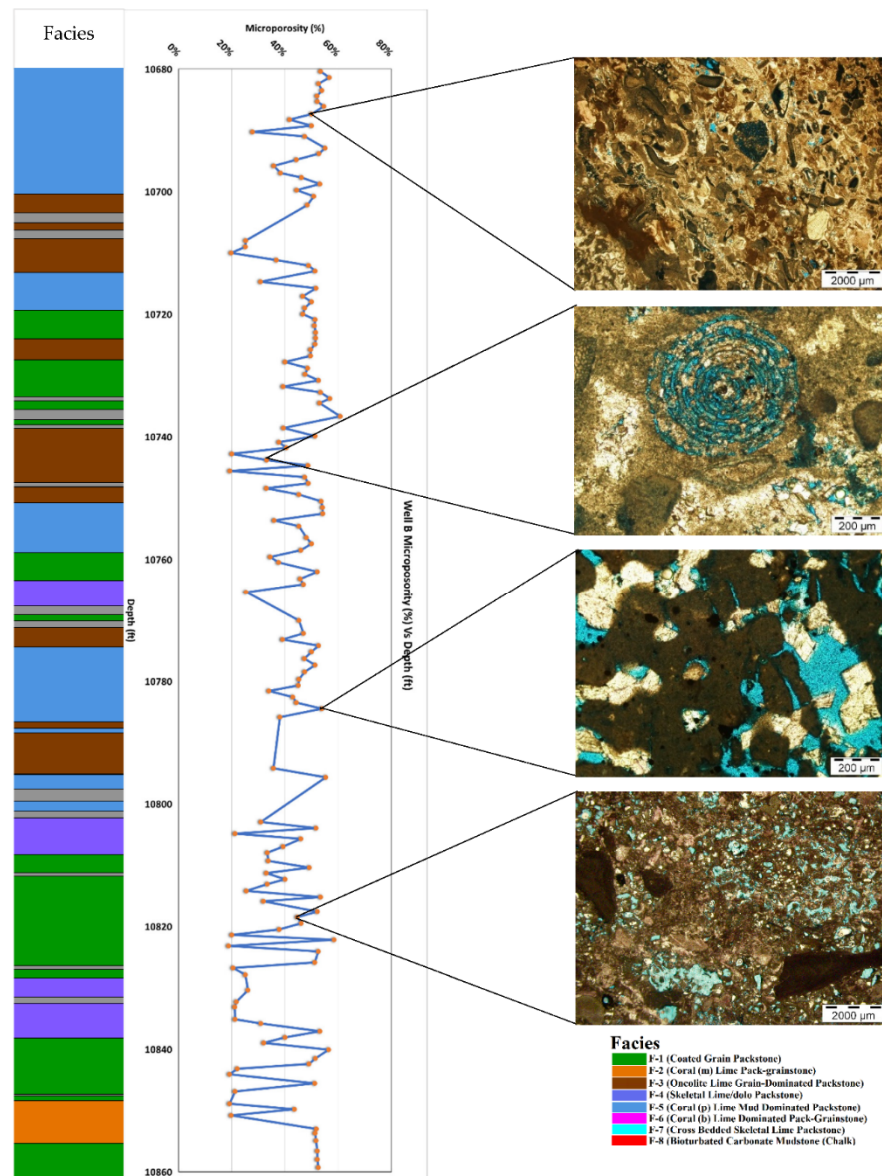


Figure 11. Macroporosity observation under transmitted light microscopy and distribution of microporosity at different depths of reservoir interval of Well A, Central Luconia, offshore, Sarawak, Malaysia.

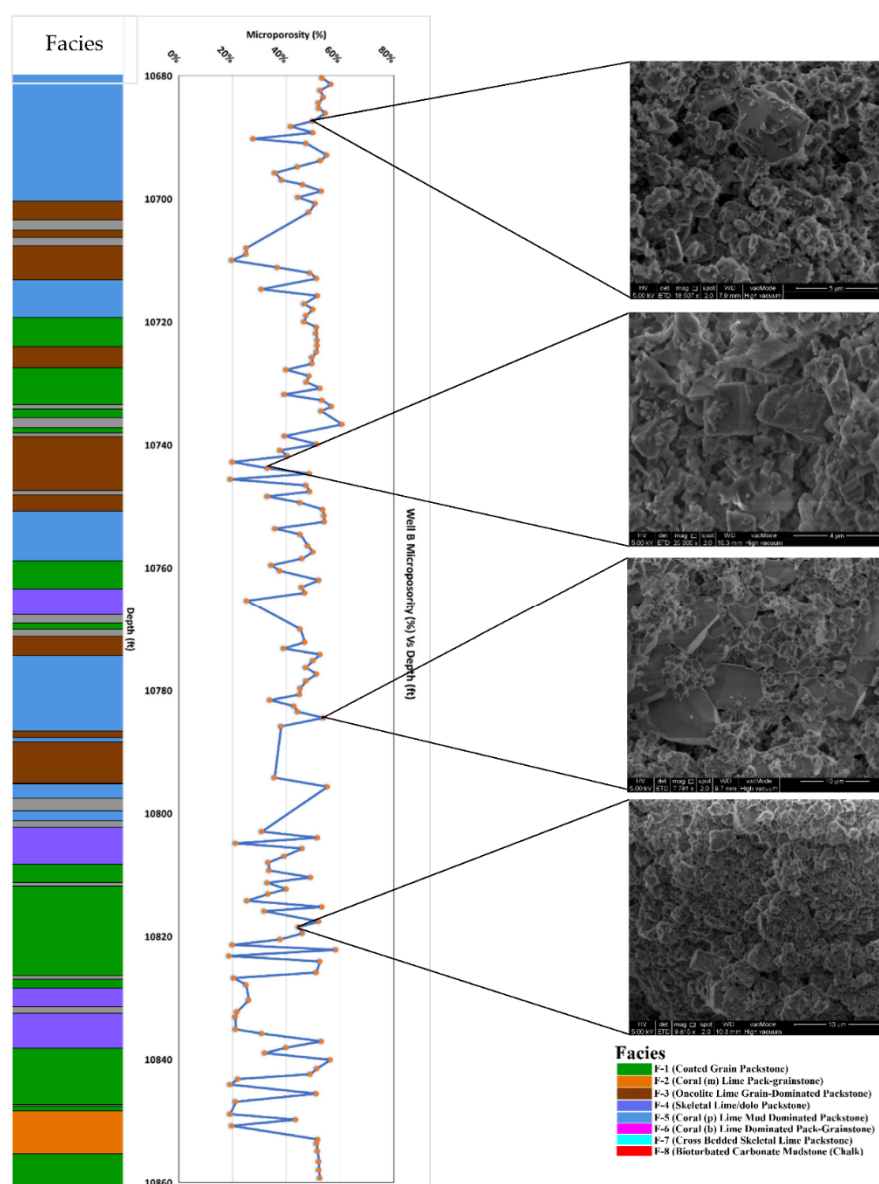


Figure 12. The observation of different microtextures with microporosity occurrence using FESEM at different depth of reservoir interval of Well A, Central Luconia, offshore, Sarawak, Malaysia.

In most cases, the relationship between porosity and permeability in carbonates is unclear. Understanding permeability behavior is critical for evaluating recoverable hydrocarbons in a reservoir because it controls fluid-flow properties [76]. Permeability is usually associated with porosity, however, when dealing with carbonate, the uncertainty is quite high due to the complicated pore structure [21,77]. The problems of porosity and permeability in hydrocarbon prediction in carbonate reservoirs have driven researchers to improve porosity and permeability correlation. Yu et al. [78], Okabe and Blunt [79], Chehrizi and Rezaee [80], Shah et al. [81] and Silin and Patzek [82] have proposed calculating permeability from porosity by classifying distinct pore types into macropores and micropores instead of focusing on total porosity. The difficulty of discerning the influence of pore types on permeability became an open challenge once the pore types were separated into macropores and micropores. The influence of microporosity on permeability was determined using data from Well A. The porosity of Well-A varies from 1% to 25% (Figure 13). By evaluating the influence of microporosity and deducing this from the total porosity indicated by the fact that the microporosity has a substantial impact on the

Miocene Luconian carbonates (Figure 13a). When compared to a cross-plot of total porosity versus permeability, the link between macroporosity and permeability has a better fit, with higher R^2 (coefficient of correlation) values. The R^2 increased from 0.58 (total porosity vs. permeability) to 0.84 (macroporosity vs. permeability) (Figure 13). Baechle, Colpaert, Eberli and Weger [31], Lucia [38], Lønøy [42] and Archie [83] concluded that the scattering points in a cross plot of porosity and permeability account for most of the carbonate pore type classifications. These scattering points are the result of qualitative descriptions of pore size, pore types, and patchiness.

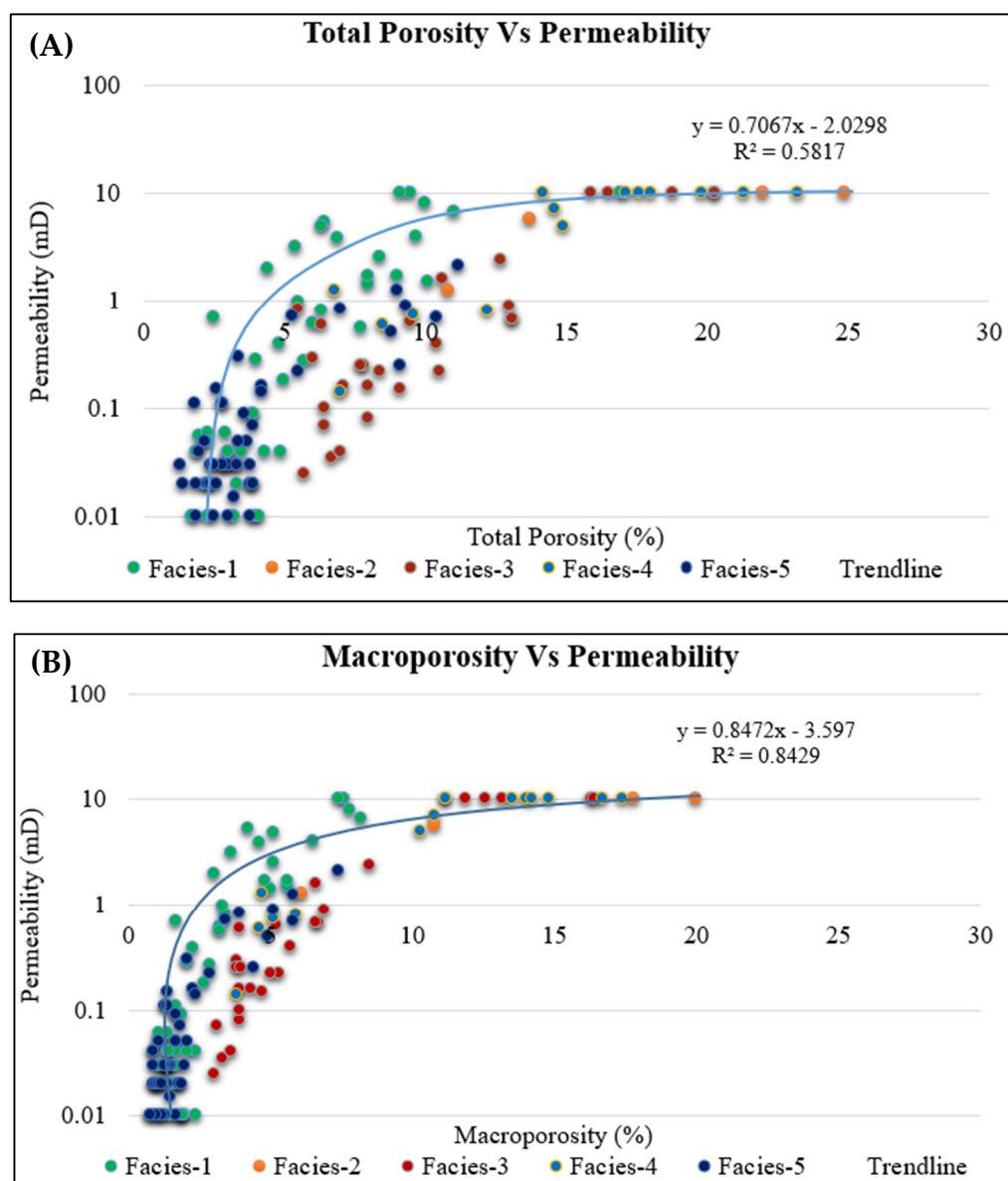


Figure 13. Total porosity, macroporosity and permeability cross plot for (A) total porosity versus permeability labelled with the different corresponding facies. The average coefficient of determination is $R^2 = 0.58\%$ (B) whereas the macroporosity versus permeability cross plot represents a better coefficient of determination which is $R^2 = 0.84\%$ in Well A Central Luconia, offshore, Sarawak, Malaysia.

It has also been suggested that the Miocene carbonates underwent a long period of diagenetic alterations [61]. As demonstrated in Figure 11, the reservoir's long diagenetic history might lead to repeated facies changes. The framework of porosity categorization may be improved by taking into consideration the pore types governed by diagenesis. The

texture and lithotype of the rock might reveal the reservoir porosity development history. Microporosity has a clear influence on permeability, as seen in Figure 13, and hence cannot be neglected.

5. Conclusions

The carbonates of Central Luconia are mostly limestone, with some dolomitic limestone. The porosity–permeability measurement shows a good porosity but low permeability value at a given total porosity, which is interpreted by the presence of high isolated mouldic pores observed under the micropores. As reported, microporosity is important when analyzing carbonate deposits. Microporosity directly impacts reservoir quality. In Central Luconia, Offshore Sarawak, Malaysia, taking macroporosity into account may improve reservoir quality predictions. Although several case studies on limestone micro-textures have been conducted, principally by Lambert, Durllet, Loreau and Marnier [2], Clerke et al. [84], Moshier [85], Domingo et al. [86] and Periere et al. [87], particle analysis and limestone petrophysical properties are required to better understand the carbonate pore system. Choquette and Pray [26] proposed a novel approach of classifying porosity that integrates pore structure and microporosity, which is essential.

Author Contributions: Conceptualization, H.T.J.; methodology, H.T.J.; software, H.T.J.; validation, H.T.J., G.K.; formal analysis, H.T.J.; investigation, H.T.J., G.K.; resources, PETRONAS, Shell, UTP; data curation, H.T.J.; writing—original draft preparation, H.T.J.; writing—review and editing, H.T.J., G.K., S.D.Z., D.M.K., A.A., A.W.; visualization, H.T.J., S.D.Z.; supervision, H.T.J.; project administration, H.T.J.; funding acquisition, G.K. All authors have read and agreed to the published version of the manuscript.

Funding: This research was funded by Yayasan University Technology PETRONAS, grant number YUTP 0153AA-A14.

Institutional Review Board Statement: Not Applicable.

Informed Consent Statement: Not Applicable.

Acknowledgments: The corresponding author would like to thank Petroliam Nasional Berhad (PETRONAS) and Sarawak Shell Berhad for kindly providing the data for this study. Deva Prasad Ghosh is acknowledged for his personal and financial support during the scientific work in the framework of the grant YUTP 0153AA-A14. HTJ would also like to thank Universiti Teknologi PETRONAS for the access to the research facilities needed for this project during his PhD study.

Conflicts of Interest: The authors declare no conflict of interest.

References

1. Janjuhah, H.T.; Alansari, A. Offshore carbonate facies characterization and reservoir quality of miocene rocks in the southern margin of south china sea. *Acta Geol. Sin.* **2020**, *94*, 1547–1561. [\[CrossRef\]](#)
2. Lambert, L.; Durllet, C.; Loreau, J.-P.; Marnier, G. Burial dissolution of micrite in Middle East carbonate reservoirs (Jurassic–Cretaceous): Keys for recognition and timing. *Mar. Pet. Geol.* **2006**, *23*, 79–92. [\[CrossRef\]](#)
3. Pal, S.; Mushtaq, M.; Banat, F.; Al Sumaiti, A.M. Review of surfactant-assisted chemical enhanced oil recovery for carbonate reservoirs: Challenges and future perspectives. *Pet. Sci.* **2018**, *15*, 77–102. [\[CrossRef\]](#)
4. Akbar, M.; Vissapragada, B.; Alghamdi, A.H.; Allen, D.; Herron, M.; Carnegie, A.; Dutta, D.; Olesen, J.-R.; Chourasiya, R.; Logan, D. A snapshot of carbonate reservoir evaluation. *Oilfield Rev.* **2000**, *12*, 20–21.
5. Han, M.; AlSofi, A.; Fuseni, A.; Zhou, X.; Hassan, S. Development of Chemical EOR Formulations for a High Temperature and High Salinity Carbonate Reservoir. In Proceedings of the IPTC 2013: International Petroleum Technology Conference, Beijing, China, 26–28 March 2013; European Association of Geoscientists & Engineers: Houten, The Netherlands, 2013; p. cp-350-00486.
6. Burchette, T.P. Carbonate rocks and petroleum reservoirs: A geological perspective from the industry. *Geol. Soc. Lond. Spec. Publ.* **2012**, *370*, 17–37. [\[CrossRef\]](#)
7. Perrin, C.; Marquez, X.; Flores, J.; Berthereau, G. Porosity depth saturation (PDS) model: Quantification of porosity preservation with burial in carbonate oil reservoirs, and application to infer oil charging time. *Mar. Pet. Geol.* **2020**, *120*, 104515. [\[CrossRef\]](#)
8. Yang, L.; Shenghe, W.; Jiagen, H.; Jianmin, L. Progress and prospects of reservoir development geology. *Pet. Explor. Dev.* **2017**, *44*, 603–614.

9. Janjuhah, H.T.; Alansari, A.; Santha, P.R. Interrelationship between facies association, diagenetic alteration and reservoir properties evolution in the Middle Miocene carbonate build up, Central Luconia, Offshore Sarawak, Malaysia. *Arab. J. Sci. Eng.* **2019**, *44*, 341–356. [\[CrossRef\]](#)
10. Janjuhah, H.T.; Alansari, A.; Vintaned, J.A.G. Quantification of microporosity and its effect on permeability and acoustic velocity in Miocene carbonates, Central Luconia, offshore Sarawak, Malaysia. *J. Pet. Sci. Eng.* **2019**, *175*, 108–119. [\[CrossRef\]](#)
11. Kontakiotis, G.; Karakitsios, V.; Cornée, J.-J.; Moissette, P.; Zarkogiannis, S.D.; Pasadakis, N.; Koskeridou, E.; Manoutsoglou, E.; Drinia, H.; Antonarakou, A. Preliminary results based on geochemical sedimentary constraints on the hydrocarbon potential and depositional environment of a Messinian sub-salt mixed siliciclastic-carbonate succession onshore Crete (Plouti section, eastern Mediterranean). *Mediterr. Geosci. Rev.* **2020**, *2*, 247–265. [\[CrossRef\]](#)
12. Janjuhah, H.T.; Sanjuan, J.; Alquadah, M.; Salah, M.K. Biostratigraphy, depositional and diagenetic processes in carbonate rocks from southern Lebanon: Impact on porosity and permeability. *Acta Geol. Sin.* **2021**, *5*, 1668–1683. [\[CrossRef\]](#)
13. Regnet, J.-B.; Fortin, J.; Nicolas, A.; Pellerin, M.; Guéguen, Y. Elastic properties of continental carbonates: From controlling factors to an applicable model for acoustic-velocity predictions. *Geophysics* **2019**, *84*, MR45–MR59. [\[CrossRef\]](#)
14. Janjuhah, H.T.; Salim, A.M.A.; Alansari, A.; Ghosh, D.P. Presence of microporosity in Miocene carbonate platform, Central Luconia, offshore Sarawak, Malaysia. *Arab. J. Geosci.* **2018**, *11*, 204. [\[CrossRef\]](#)
15. Peng, S. Gas relative permeability and its evolution during water imbibition in unconventional reservoir rocks: Direct laboratory measurement and a conceptual model. *SPE Reserv. Eval. Eng.* **2019**, *22*, 1346–1359. [\[CrossRef\]](#)
16. Bashir, Y.; Babasafari, A.A.; Biswas, A.; Hamidi, R.; Moussavi Alashloo, S.Y.; Tariq Janjua, H.; Prasad Ghosh, D.; Weng Sum, C. Cohesive Approach for High-Resolution Seismic Using Inversion & Imaging in Malaysian Carbonate Field. In Proceedings of the International Petroleum Technology Conference, Beijing, China, 26–28 March 2019.
17. Janjuhah, H.T.; Salim, A.; Mohammad, A.; Ali, M.Y.; Ghosh, D.P.; Hassan, A.; Hakif, M. Development of Carbonate Buildups and Reservoir Architecture of Miocene Carbonate Platforms, Central Luconia, Offshore Sarawak, Malaysia. In Proceedings of the SPE/IATMI Asia Pacific Oil & Gas Conference and Exhibition, Jakarta, Indonesia, 17–19 October 2017.
18. Norbistrath, J.H.; Weger, R.J.; Eberli, G.P. Complex resistivity spectra and pore geometry for predictions of reservoir properties in carbonate rocks. *J. Pet. Sci. Eng.* **2017**, *151*, 455–467. [\[CrossRef\]](#)
19. Kontakiotis, G.; Moforis, L.; Karakitsios, V.; Antonarakou, A. Sedimentary facies analysis, reservoir characteristics and paleogeography significance of the early jurassic to eocene carbonates in epiros (Ionian Zone, Western Greece). *J. Mar. Sci. Eng.* **2020**, *8*, 706. [\[CrossRef\]](#)
20. Chacko, S.; Fainstein, R.; Li, C. Introduction to this special section: Southeast Asia. *Lead. Edge* **2020**, *39*, 541–542. [\[CrossRef\]](#)
21. Janjuhah, H.T.; Alansari, A.; Ghosh, D.P.; Bashir, Y. New approach towards the classification of microporosity in Miocene carbonate rocks, Central Luconia, offshore Sarawak, Malaysia. *J. Nat. Gas Geosci.* **2018**, *3*, 119–133. [\[CrossRef\]](#)
22. Folk, R.L. Practical petrographic classification of limestones. *AAPG Bull.* **1959**, *43*, 1–38.
23. Dunham, R.J. Classification of carbonate rocks according to depositional textures. *Am. Assoc. Pet. Geol.* **1962**, *1*, 108–121.
24. Embry, A.F.; Klován, J.E. A late Devonian reef tract on northeastern Banks Island, NWT. *Bull. Can. Pet. Geol.* **1971**, *19*, 730–781.
25. Wardlaw, N. Pore geometry of carbonate rocks as revealed by pore casts and capillary pressure. *AAPG Bull.* **1976**, *60*, 245–257.
26. Choquette, P.W.; Pray, L.C. Geologic nomenclature and classification of porosity in sedimentary carbonates. *AAPG Bull.* **1970**, *54*, 207–250.
27. Moore, C.H. *Carbonate Diagenesis and Porosity*; Elsevier: Amsterdam, The Netherlands, 1989; Volume 46.
28. Maliva, R.G. Carbonate Facies Models and Diagenesis. In *Aquifer Characterization Techniques*; Springer: Berlin/Heidelberg, Germany, 2016; pp. 91–110.
29. Fabricius, I.L.; Røgen, B.; Gommessen, L. How depositional texture and diagenesis control petrophysical and elastic properties of samples from five North Sea chalk fields. *Pet. Geosci.* **2007**, *13*, 81–95. [\[CrossRef\]](#)
30. Fabricius, I.L.; Bächle, G.T.; Eberli, G.P. Elastic moduli of dry and water-saturated carbonates—Effect of depositional texture, porosity, and permeability. *Geophysics* **2010**, *75*, N65–N78. [\[CrossRef\]](#)
31. Bächle, G.T.; Colpaert, A.; Eberli, G.P.; Weger, R.J. Effects of microporosity on sonic velocity in carbonate rocks. *Lead. Edge* **2008**, *27*, 1012–1018. [\[CrossRef\]](#)
32. Anselmetti, F.S.; Eberli, G.P. Controls on Sonic Velocity in Carbonates. In *Experimental Techniques in Mineral and Rock Physics*; Springer: Berlin/Heidelberg, Germany, 1993; pp. 287–323.
33. Melim, L.A.; Anselmetti, F.S.; Eberli, G.P. The importance of pore type on permeability of Neogene carbonates, Great Bahama Bank. In *Subsurface Geology of a Prograding Carbonate Platform Margin, Great Bahama Bank: Results of the Bahamas Drilling Project*; SEPM: Tulsa, OK, USA, 2001; Volume 70, pp. 217–238.
34. Anselmetti, F.S.; Eberli, G.P. The velocity-deviation log: A tool to predict pore type and permeability trends in carbonate drill holes from sonic and porosity or density logs. *AAPG Bull.* **1999**, *83*, 450–466.
35. Weger, R.J.; Eberli, G.P.; Bächle, G.T.; Massaferrro, J.L.; Sun, Y.-F. Quantification of pore structure and its effect on sonic velocity and permeability in carbonates. *AAPG Bull.* **2009**, *93*, 1297–1317. [\[CrossRef\]](#)
36. Kumar, M.; Han, D.-h. Pore Shape Effect on Elastic Properties of Carbonate Rocks. In *Proceedings of the 2005 SEG Annual Meeting*; Society of Exploration Geophysicists: Houston, TX, USA, 2005.
37. Fitch, P.J.; Lovell, M.A.; Davies, S.J.; Pritchard, T.; Harvey, P.K. An integrated and quantitative approach to petrophysical heterogeneity. *Mar. Pet. Geol.* **2015**, *63*, 82–96. [\[CrossRef\]](#)

38. Lucia, F.J. Rock-fabric/petrophysical classification of carbonate pore space for reservoir characterization. *Am. Assoc. Pet. Geol.* **1995**, *79*, 1275–1300.
39. Anselmetti, F.S.; Eberli, G.P. *Sonic Velocity in Carbonate—A Product of Original Composition and Postdepositional Porosity Evolution*; Ann: AAPG-SEPMEMD-DPA-CSPG; Conv. Abstracts; American Association of Petroleum Geologists: Tulsa, OK, USA, 1992.
40. Pittman, E.D. Relationship of porosity and permeability to various parameters derived from mercury injection-capillary pressure curves for sandstone (1). *AAPG Bull.* **1992**, *76*, 191–198.
41. Cantrell, D.L.; Hagerty, R.M. Microporosity in Arab formation carbonates, Saudi Arabia. *GeoArabia* **1999**, *4*, 129–154. [[CrossRef](#)]
42. Lønøy, A. Making sense of carbonate pore systems. *AAPG Bull.* **2006**, *90*, 1381–1405. [[CrossRef](#)]
43. Lucia, F.; Loucks, R. Microporosity in carbonate mud: Early development and petrophysics. *Gulf Coast Assoc. Geol. Societies* **2013**, *2*, 1275–1300.
44. Jobe, T.; Sarg, J. Microporosity Characterization of Mud-Rich Carbonate Rocks. In *Pore Scale Phenomena: Frontiers in Energy and Environment*; World Scientific: Singapore, 2015; pp. 67–89.
45. Archie, G.E. Classification of carbonate reservoir rocks and petrophysical considerations. *Aapg Bull.* **1952**, *36*, 278–298.
46. Tucker, M.E.; Wright, V.P. *Carbonate Sedimentology*; John Wiley & Sons: New York, NY, USA, 2009.
47. Wilson, J.C.; McBride, E.F. Compaction and porosity evolution of Pliocene sandstones, Ventura Basin, California. *AAPG Bull.* **1988**, *72*, 664–681.
48. Wilson, M.E. Global and regional influences on equatorial shallow-marine carbonates during the Cenozoic. *Palaeogeogr. Palaeoclimatol. Palaeoecol.* **2008**, *265*, 262–274. [[CrossRef](#)]
49. Scholle, P.A.; Ulmer-Scholle, D.S. *A Color Guide to the Petrography of Carbonate Rocks: Grains, Textures, Porosity, Diagenesis*, AAPG Memoir 77; AAPG: Tulsa, OK, USA, 2003; Volume 77.
50. Al-Dabbas, M.; Al-Jassim, J.; Al-Jumaily, S. Depositional environments and porosity distribution in regressive limestone reservoirs of the Mishrif Formation, Southern Iraq. *Arab. J. Geosci.* **2010**, *3*, 67–78. [[CrossRef](#)]
51. Purser, B.; Brown, A.; Aissaoui, D. Nature, Origin and Evolution of Porosity in Dolomites. In *Dolomites: A Volume in Honour of Dolomieu*; Purser, B., Tucker, M., Zenger, D., Eds.; Special Publication; International Association of Sedimentologists: Algiers, Algeria, 1994; pp. 283–308.
52. Xi, K.; Cao, Y.; Jähren, J.; Zhu, R.; Bjørlykke, K.; Haile, B.G.; Zheng, L.; Hellevang, H. Diagenesis and reservoir quality of the Lower Cretaceous Quantou Formation tight sandstones in the southern Songliao Basin, China. *Sediment. Geol.* **2015**, *330*, 90–107. [[CrossRef](#)]
53. Madden, R.H.; Wilson, M.E. Diagenesis of a SE Asian Cenozoic carbonate platform margin and its adjacent basinal deposits. *Sediment. Geol.* **2013**, *286*, 20–38. [[CrossRef](#)]
54. Wilson, J.L. *Carbonate Facies in Geologic History*; Springer Science & Business Media: Berlin/Heidelberg, Germany, 2012.
55. Lucia, F. Petrophysical parameters estimated from visual descriptions of carbonate rocks: A field classification of carbonate pore space. *J. Pet. Technol.* **1983**, *35*, 629–637. [[CrossRef](#)]
56. Rahman, M.H.; Pierson, B.J.; Yusoff, W.; Ismail, W. Classification of Microporosity in Carbonates: Examples from Miocene Carbonate Reservoirs of Central Luconia, Offshore Sarawak, Malaysia. In *Proceedings of the International Petroleum Technology Conference*; European Association of Geoscientists & Engineers: Houten, The Netherlands, 2011.
57. Rahman, M.H.; Pierson, B.J. Effects of Microporosity on Permeability and Sonic Velocity of Miocene Carbonates and an Approach to Relate Micrite Microtextures with Microporosity Occurrences in Miocene Carbonate Reservoirs of Offshore Sarawak, Malaysia. In *SEG Technical Program Expanded Abstracts 2011*; Society of Exploration Geophysicists: Tulsa, OK, USA, 2011; pp. 2059–2063.
58. Nole, M.; Daigle, H.; Milliken, K.L.; Prodanović, M. A method for estimating microporosity of fine-grained sediments and sedimentary rocks via scanning electron microscope image analysis. *Sedimentology* **2016**, *63*, 1507–1521. [[CrossRef](#)]
59. Kaczmarek, S.E.; Fullmer, S.M.; Hasiuk, F.J. A universal classification scheme for the microcrystals that host limestone microporosity. *J. Sediment. Res.* **2015**, *85*, 1197–1212. [[CrossRef](#)]
60. Wentworth, C.K. A scale of grade and class terms for clastic sediments. *J. Geol.* **1922**, *30*, 377–392. [[CrossRef](#)]
61. Janjuhah, H.T.; Salim, A.M.A.; Ghosh, D.P. Sedimentology and reservoir geometry of the Miocene Carbonate deposits in Central Luconia, Offshore, Sarawak, Malaysia. *J. Appl. Sci.* **2017**, *17*, 153–170. [[CrossRef](#)]
62. Lucia, F.J. *Carbonate Reservoir Characterization: An Integrated Approach*; Springer: Berlin/Heidelberg, Germany; New York, NY, USA, 2007.
63. Zhuravlev, A.Y.; Wood, R.A. Controls on carbonate skeletal mineralogy: Global CO₂ evolution and mass extinctions. *Geology* **2009**, *37*, 1123–1126. [[CrossRef](#)]
64. Pittman, E.D. Microporosity in carbonate rocks: Geological notes. *AAPG Bull.* **1971**, *55*, 1873–1878.
65. Ong, C.W.; Ho, P.; Leo, H.L. Effects of microporous stent graft on the descending aortic aneurysm: A patient-specific computational fluid dynamics study. *Artif. Organs* **2016**, *40*, E230–E240. [[CrossRef](#)]
66. Anselmetti, F.S.; Luthi, S.; Eberli, G.P. Quantitative characterization of carbonate pore systems by digital image analysis. *Am. Assoc. Pet. Geol. Bull.* **1998**, *82*, 1815–1836.
67. Ruzyla, K.; Jezek, D. Staining method for recognition of pore space in thin and polished sections: Research method paper. *J. Sediment. Res.* **1987**, *57*, 777–778. [[CrossRef](#)]
68. Yanguas, J.; Dravis, J.J. Blue fluorescent dye technique for recognition of microporosity in sedimentary rocks: Research method paper. *J. Sediment. Res.* **1985**, *55*, 600–602.

-
69. Milliken, K.L.; Curtis, M.E. Imaging pores in sedimentary rocks: Foundation of porosity prediction. *Mar. Pet. Geol.* **2016**, *73*, 590–608. [[CrossRef](#)]
 70. Arribas, M.; Bustillo, A.; Tsige, M. Lacustrine chalky carbonates: Origin, physical properties and diagenesis (Palaeogene of the Madrid Basin, Spain). *Sediment. Geol.* **2004**, *166*, 335–351. [[CrossRef](#)]
 71. Cox, P.; Wood, R.; Dickson, J.; Al Rougha, H.; Shebl, H.; Corbett, P. Dynamics of cementation in response to oil charge: Evidence from a Cretaceous carbonate field, UAE. *Sediment. Geol.* **2010**, *228*, 246–254. [[CrossRef](#)]
 72. Flugel, E. *Microfacies of Carbonate Rocks: Analysis, Interpretation and Application*; Springer: Berlin/Heidelberg, Germany; New York, NY, USA, 2004; p. 979.
 73. Kaldi, J. Diagenetic microporosity (chalky porosity), middle Devonian Kee Scarp reef complex, Norman wells, northwest territories, Canada. *Sediment. Geol.* **1989**, *63*, 241–252. [[CrossRef](#)]
 74. Volery, C.; Davaud, E.; Foubert, A.; Caline, B. Lacustrine microporous micrites of the Madrid Basin (Late Miocene, Spain) as analogues for shallow-marine carbonates of the Mishrif reservoir Formation (Cenomanian to Early Turonian, Middle East). *Facies* **2010**, *56*, 385–397. [[CrossRef](#)]
 75. Morad, D.; Paganoni, M.; Al Harthi, A.; Morad, S.; Ceriani, A.; Mansurbeg, H.; Al Suwaidi, A.; Al-Aasm, I.S.; Ehrenberg, S.N. Origin and evolution of microporosity in packstones and grainstones in a Lower Cretaceous carbonate reservoir, United Arab Emirates. *Geol. Soc. Lond. Spec. Publ.* **2016**, *435*, 47–66. [[CrossRef](#)]
 76. Van Geet, M.; Swennen, R.; Durmishi, C.; Roure, F.; Muchez, P. Paragenesis of Cretaceous to Eocene carbonate reservoirs in the Ionian fold and thrust belt (Albania): Relation between tectonism and fluid flow. *Sedimentology* **2002**, *49*, 697–718. [[CrossRef](#)]
 77. Ehrenberg, S. Porosity destruction in carbonate platforms. *J. Pet. Geol.* **2006**, *29*, 41–52. [[CrossRef](#)]
 78. Yu, Y.; Visser, F.; Amro, M.M. Quantitative Effect of Microporosity on Permeability in Carbonate Reservoirs. In Proceedings of the International Petroleum Technology Conference, Kuala Lumpur, Malaysia, 10–12 December 2014.
 79. Okabe, H.; Blunt, M. Predicting Permeability through 3D Pore-Space Images Reconstructed Using Multiple-Point Statistics. In Proceedings of the International Symposium of the Society of Core Analysts, Abu Dhabi, United Arab Emirates, 5–9 October 2004; pp. 5–9.
 80. Chehrizi, A.; Rezaee, R. A systematic method for permeability prediction, a Petro-Facies approach. *J. Pet. Sci. Eng.* **2012**, *82*, 82–83, 1–16. [[CrossRef](#)]
 81. Shah, S.; Yang, J.; Crawshaw, J.P.; Gharbi, O.; Boek, E.S. Predicting Porosity and Permeability of Carbonate rocks from Core-scale to Pore-Scale using Medical CT, Confocal Laser Scanning Microscopy and Micro CT. In Proceedings of the SPE Annual Technical Conference and Exhibition, New Orleans, LS, USA, 20 September–2 October 2013.
 82. Silin, D.B.; Patzek, T.W. Predicting Relative-Permeability Curves Directly from Rock Images. In Proceedings of the SPE Annual Technical Conference and Exhibition, New Orleans, LS, USA, 4–7 October 2009.
 83. Archie, G.E. The electrical resistivity log as an aid in determining some reservoir characteristics. *Trans. AIME* **1942**, *146*, 54–62. [[CrossRef](#)]
 84. Clerke, E.A.; Mueller, H.; Phillips, E.C.; Eyvazzadeh, R.Y.; Jones, D.H.; Ramamoorthy, R.; Srivastava, A. Application of Thomeer Hyperbolas to decode the pore systems, facies and reservoir properties of the Upper Jurassic Arab D Limestone, Ghawar field, Saudi Arabia: A “Rosetta Stone” approach. *GeoArabia* **2008**, *13*, 113–160. [[CrossRef](#)]
 85. Moshier, S.O. Development of microporosity in a micritic limestone reservoir, Lower Cretaceous, Middle East. *Sediment. Geol.* **1989**, *63*, 217–240. [[CrossRef](#)]
 86. Domingo, C.; García-Carmona, J.; Loste, E.; Fanovich, A.; Fraile, J.; Gómez-Morales, J. Control of calcium carbonate morphology by precipitation in compressed and supercritical carbon dioxide media. *J. Cryst. Growth* **2004**, *271*, 268–273. [[CrossRef](#)]
 87. Periere, M.D.; Durllet, C.; Vennin, E.; Lambert, L.; Bourillot, R.; Caline, B.; Poli, E. Morphometry of micrite particles in cretaceous microporous limestones of the Middle East: Influence on reservoir properties. *Mar. Pet. Geol.* **2011**, *28*, 1727–1750. [[CrossRef](#)]